ELSEVIER

Polymer 43 (2002) 5139–5145

polymer

www.elsevier.com/locate/polymer

Study of oriented block copolymers films obtained by roll-casting

Marcelo A. Villar[a,1], Daniel R. Rueda[b], Fernando Ania[b], Edwin L. Thomas[a,*]

[a]*Department of Materials Science and Engineering, Massachusetts Institute of Technology, Room 13-5094, 77 Massachusetts Avenue, Cambridge, MA 02139, USA*

[b]*Instituto de Estructura de la Materia, CSIC, Serrano 119, 28006 Madrid, Spain*

Received 11 January 2002; received in revised form 3 June 2002; accepted 5 June 2002

Abstract

Roll-casting orientation of cylinder microphase separated poly(styrene-*b*-butadiene-*b*-styrene) triblock copolymers, was analyzed. The mechanical anisotropy of roll-cast films, defined as the ratio of Young's modulus obtained parallel and perpendicular to poly(styrene) cylinders, is similar for samples prepared using a dimensionless minimum gap between rolls higher than approximately 0.02. The orientation of samples was also characterized by measuring the full width at the half intensity maximum of small angle X-ray scattering intensity circle profiles and showed good correlation with modulus measurements. Blends of triblock and diblock with up to 60 wt% of diblock show orientation as good as the neat triblock sample.

Keywords: Roll-casting; Oriented block copolymers; Small angle X-ray scattering

1. Introduction

Block copolymers composed of incompatible block segments generally form a microdomain structure in the solid state as a consequence of microphase separation of the constituent block chains. For flexible chain non-crystalline diblock copolymer melts, body centered-cubic array of spheres, hexagonal arrays of cylinders, bicontinuous double gyroid domains, and lamellar structures are observed by changing the volume fraction of the two components. Materials composed of cylindrical or lamellar microdomains present a local anisotropy. On the nanometer scale, the structure within the grains is ordered, however, in practice the whole sample displays isotropic properties since the small grains are randomly oriented over the whole specimen. External forces such as those induced by flow [1–4] and electric fields [5,6] at temperatures above the glass transition temperature of all components, in a molten but microphase separated state, have been shown to induce a global alignment of the block copolymer microstructure.

Different groups have been working on the orientation of diblock and triblock copolymers in order to obtain globally oriented microdomain structures on a large scale constituting a 'single-crystal' structure. Keller et al. [1] prepared, in the early 1970s, polystyrene (PS) cylinders oriented in a polybutadiene (PB) matrix by extruding a poly(styrene-*b*-butadiene-*b*-styrene) (SBS) triblock copolymer through an orifice at 100–120 °C into a tube of cylindrical or rectangular cross-section. Annealing of the samples leads to greater perfection of microdomain packing. Subsequently, Hadziioannou et al. [3] introduced a new way of orienting block copolymers based on the reciprocating motion of two parallel metal plates. This procedure has been recently used to obtain oriented diblock copolymers [7]. A similar method, based on large amplitude oscillatory shear (LAOS), was introduced by Morrison and Winter [4] to orient triblock copolymers using a stress rheometer with a cone and plate geometry. The LAOS technique has been extensively used to understand the orientation of block copolymers with lamellar structure [8–14] and, to a less extent, of block copolymers forming a hexagonally ordered cylindrical microstructure [15,16]. On the other hand, an electric field has also been used to align poly(styrene-*b*-isoprene) (PS/PI) [5] and poly(styrene-*b*-methylmethacrylate) (PS/PMMA) [6] diblock copolymers either from solution or in the melt state.

Albalak and Thomas [17–20] presented a new technique of orienting block copolymers using a device based on a

* Corresponding author. Tel.: +1-617-253-6901; fax: +1-617-253-4119.
E-mail addresses: elt@mit.edu (E.L. Thomas), mvillar@plapiqui.edu.ar (M.A. Villar).
[1] Present address: Planta Piloto de Ingeniería Química, PLAPIQUI (UNS-CONICET), CC 717 (8000) Bahía Blanca, Argentina. Tel./fax: +54-291-486-1700.

0032-3861/01/$ - see front matter
PII: S0032-3861(02)00388-9

novel casting method termed 'roll-casting'. In this method, polymer solutions are subjected to a flow field between two counter-rotating rolls while at the same time the solvent is evaporated. During processing, the block copolymers microphase separate into macroscopically oriented films. The flow field also plays, in this case, an important role in the orientation.

The aim of this paper is to study the influence of processing conditions as well as diblock content on the degree of orientation of cylindrical PS microdomain of triblock PS/PB/PS as revealed by the anisotropy in the mechanical properties and in the small angle X-ray patterns.

2. Experimental

Materials used in the present study were commercial poly(styrene-*b*-butadiene-*b*-styrene) (SBS) triblock copolymers provided by Shell Chemical Co. and by DEXCO Co. Shell materials have been shown to be a mixture of homopolystyrene (PS), poly(styrene-*b*-butadiene) diblock (SB) and poly(styrene-*b*-butadiene-*b*-styrene) (SBS) triblock [21]. On the other hand, DEXCO materials were found to be more than 99% triblock [21]. Table 1 shows compositions and molecular weights of the copolymers used. A series of blends of a pure diblock (SB) and a pure triblock (SBS) from DEXCO were also studied. Blends containing about 20, 40, and 60 wt% of diblock were prepared by dissolving both polymers in cumene. Table 2 shows the nomenclature used for the blends as well as the weight fraction of diblock and triblock copolymer and the overall styrene weight fraction, which is maintained almost constant for all the blends. Initial solutions were made using approximately 100 g of polymer in 200 ml of cumene (0.33 g/ml). Cumene was chosen as a solvent because it is nearly a non-preferential solvent for the styrene and butadiene blocks and because it has a low vapor pressure that permits slow solvent evaporation.

The experimental system used in this work, consisting of two counter-rotating rolls, is the same type typically utilized in conventional calenders or roll-mills [17]. The polymer solution flows, in both cases, between two adjacent cylinders. It is compressed and forced to flow through the nip of the rolls (minimum distance between the rolls), denoted $2H_0$ (Fig. 1). After passing the nip, the material fills the gap between the rolls for some time, until the material leaves the rolls coating either one or both of them.

The experiments begin with a solution whose microphase separates during the flow process as a result of evaporation of the solvent. During processing it is possible to distinguish two different regimes. Before the order–disorder concentration (ODC), the flow field is acting on molecules which are more or less entangled but free to move. Considering the molecular weight between entanglements and the molecular weight of the respective blocks, polybutadiene blocks are well entangled while

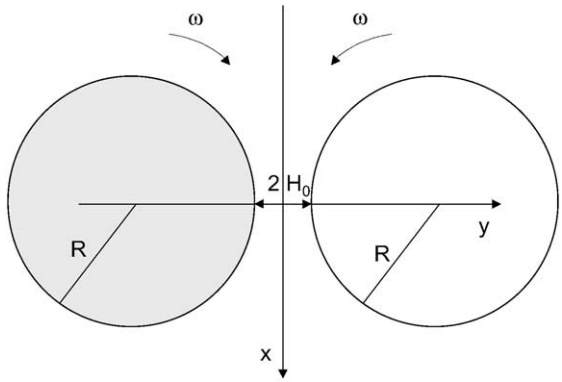

Fig. 1. Schematic representation of the roll-casting apparatus. The rolls rotate at the same angular velocity, ω. The minimum gap width $2H_0$ in the system, called 'the nip', is also indicated. Axis notation: x-axis is the flow direction (tangential to the rollers), y-axis is the gradient direction (radial to the rollers), and z-axis is the neutral direction.

polystyrene blocks are not. After microphase separation occurs the flow field now acts on the microdomain morphology, which in our case is PS cylinders (glass-like at room temperature in the absence of solvent) in a rubbery PB matrix. Depending on the processing conditions, polystyrene cylinders are found to be well oriented parallel to the flow direction (i.e. along x) and are uniformly packed in a near single-crystal hexagonal texture [17].

In the previous roll-casting work both rotating cylinders were made of aluminum which often resulted in fragmentation of the polymer film onto both rolls. This problem was solved by using different materials for each cylinder. In the current setup one cylinder was made of stainless steel while the second one has a polytetrafluoroethylene (Teflon®) coating [17]. In this new system, after sufficient solvent evaporation, the film transfers onto the metal roll due to its higher surface tension [22]. Two cylinder diameters were used: 0.01905 m (3/4 in.) and 0.0762 m (3 in.). However, most of the films studied were obtained with the smaller cylinders. The polymer solutions were typically rolled for 5–6 h and the resulting films were dried on the roll overnight. Once removed from the roll, the films were vacuum-dried at 40–50 °C for a week and annealed at 130 °C for another week. Fig. 2 shows a schematic representation of the poly(styrene) cylinders in the poly(butadiene) matrix.

A Model 4501 Instron Tensile Testing Instrument was employed to determine the mechanical behavior of roll-cast films. 'Dog-bone' specimens (length: 5 cm, width: 0.5 cm, and thickness: 0.2–1 cm) were cut parallel and perpendicular to the flow (x-direction). The stress–strain curve behavior was obtained in both directions, parallel and perpendicular to the cylinder axes, using a deformation speed of 0.04 m/min.

A RU-120 X-ray generator with rotating Cu anode working at 40 kV and 120 mA, with fine focus, was used to

Table 1
Materials used

Polymer (trade name)	Total styrene weight fraction	hPS weight fraction	SB weight fraction	SBS weight fraction	hPS molecular weight	SB molecular weight	SBS molecular weight	Copolym. styrene weight fraction
D-1102[a]	0.28	0.02	0.27	0.71	11,000	41,500	83,000	0.265
8550-D[b]	0.28	–	–	>0.99	–	–	80,000	0.28
2320-D[b]	0.25	–	>0.99	–	–	72,000	–	0.25

[a] Kraton Co.
[b] DEXCO Co.

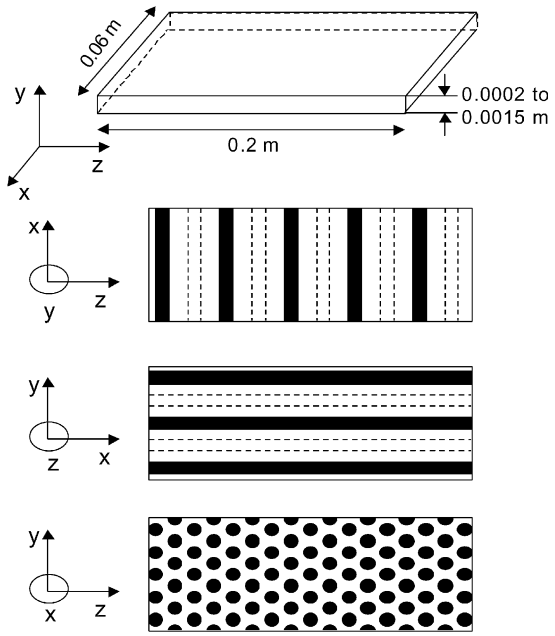

Fig. 2. Schematic representation of the hexagonally packed poly(styrene) cylinders obtained by the roll-casting process. Axis notation is the same as in Fig. 1.

record the small angle X-ray scattering (SAXS) patterns by means of a Rigaku camera with point collimation coupled to a CCD area detector. A sample-detector distance of 0.6 m was used. Strips along the x and z directions, about 1 mm thick (y-direction), were cut from the films in order to take X-ray patterns in the two directions orthogonal to the strip length (i.e. the X-ray beam is, respectively, parallel to the y and x directions when a z-strip is used). The resolution of the area detector is 0.093 mm/pixel. The sample scattering under these conditions typically yields count rates of about 100 cps. To improve the statistics and quality of SAXS patterns accumulation times of about 1 h were required. The SAXS patterns were orientationally analyzed by means of circular profiles throughout the intensity maximum of concentric reflections.

3. Results and discussion

3.1. Mechanical properties

The mechanical properties of the roll-cast films is, perhaps, the most interesting consequence of the near single-crystal characteristics of the samples. As a consequence of the structure an extremely high degree of mechanical anisotropy can be expected [23–25]. In order to examine this behavior, specimens for tensile testing were cut from the annealed films using a dog-bone-shaped template with the long dimension parallel and perpendicular to the flow direction.

Fig. 3 shows the typical stress–strain behavior of the oriented SBS specimens measured at room temperature. The

Table 2
Blends prepared by solution mixing of a diblock SB (2320-D) and a triblock SBS (8550-D) copolymer

Blend	SB weight fraction	SBS weight fraction	Total styrene weight fraction
B 0-100	–	>0.99	0.280
B 20-80	0.216	0.784	0.274
B 40-60	0.402	0.598	0.268
B 60-40	0.598	0.402	0.262
B 100-0	>0.99	–	0.250

tensile stress on the ordinate refers to the nominal engineering stress, i.e. tensile force divided by original cross-sectional area of the specimen. In the parallel direction (deformation of the sample parallel to the PS cylinders) the material yields at low deformation (around 3% strain) beyond which the load drops slightly. The load remains constant as a neck propagates along the specimen and when the sample has completely necked the load again increases and the further deformation is elastic [2]. If the deformation is applied perpendicular to the PS cylinders, the hexagonal array of cylinders is progressively deformed up to 20% strain. In this range of strain the lattice strain was found to be indistinguishable from the macroscopic sample strain. Beyond 20% strain the correspondence between lattice and sample strain is progressively lost and the applied strain is only partially recoverable [23,25].

Parallel and perpendicular Young's modulus ($E_{\|}$ and $E_{\perp}$) for commercial materials as well as for the blends were obtained from the stress–strain curves and are shown in Fig. 4(a) and (b). The values of $E_{\perp}$ are in very good agreement with those reported in the literature. However, the values of $E_{\|}$ are lower than those obtained by Odell and Keller [23]. The difference with the values reported in the literature may arise from different sources of error: the alignment of the axis of the dog-bone specimens with the average cylinder axis direction, the precision of the measurement of the gauge length and strain in the small strain region for this highly anisotropic sample and the velocity of deformation used. As Odell and Keller [23] pointed out, highly anisotropic materials present special problems in the determination of elastic modulus. Despite a possible imprecision of the Young's modulus along the stiff direction, a good estimation of the orientation of the microstructure in the films is given by the ratio of parallel and perpendicular modulus. Fig. 4(c) shows $E_{\|}/E_{\perp}$ values for the materials studied in the present work as a function of processing parameters. The commercial materials as well as the blends containing approximately 27 wt% of PS present a good orientation if the ratio of gap clearance to roll radius is higher than 0.02. When the value of the nip to roll radius ratio is lower than 0.02 the shear rate at the wall increases and this can be the cause of the poor orientation in the films.

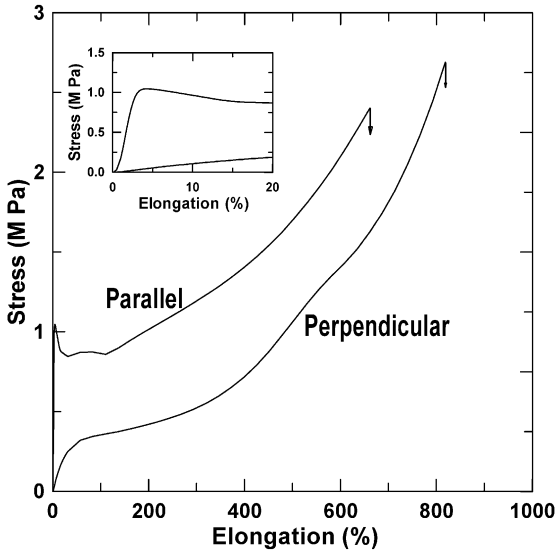

Fig. 3. Stress–strain curves, measured at room temperature, for an oriented SBS specimen deformed in the parallel direction (along x-direction, deformation parallel to the PS cylinders), and in the perpendicular direction (along z-direction, deformation perpendicular to the PS cylinders).

3.2. Small angle X-ray scattering

Fig. 5(a)–(c) shows the X-ray patterns, recorded with the X-ray beam perpendicular to the zy, zx and xy planes, respectively, for an oriented sample of SBS (DEXCO 8550-D, thickness 0.62 mm). Fig. 5(a) shows the hexagonal symmetry of reflections. The reflections can be classified according to their radial value, q. From this value, the corresponding lattice spacing, d, can be calculated from Bragg's law. It is remarkable that the very strong intensity of the smallest angle reflection, q_1, appears at very short (few seconds) time exposure of the sample. This helped in checking the proper alignment of the strip sample. A very small tilting of the sample around its x-direction produces large differences in the intensity of the reflections at some q, including even the disappearance of some reflections. Having in mind the geometry for the hexagonal packing, the longest spacing (first circle reflections, q_1) are related to the minimum distance between layers containing the diffracting objects. The reflections of the second circle q_2 would be related to the real distance between two diffracting objects. This distance is taken as the parameter axis a of the hexagonal lattice. Table 3 shows the calculated spacings d_1, d_2, and the parameters a for some of the films prepared from the blends listed in Table 2. The a values increase up to about 15% with an increasing concentration of the diblock SB component up to 40 wt% in the blend.

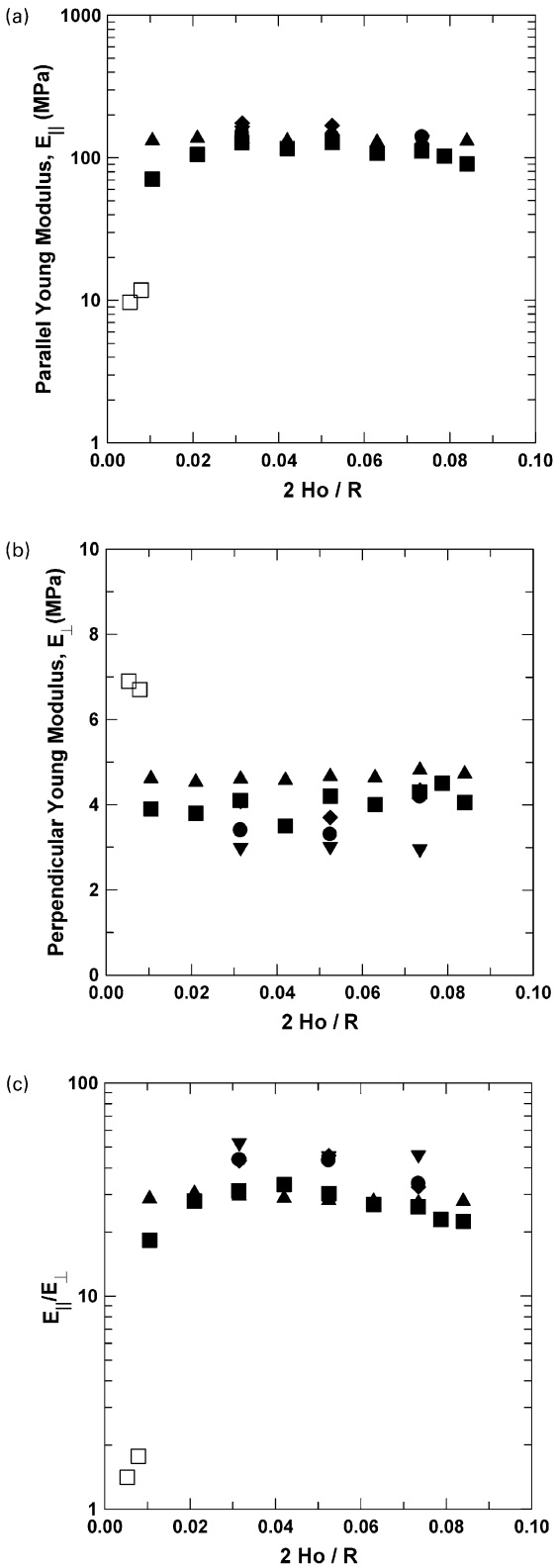

Fig. 4. (a) Parallel Young's modulus, (b) Perpendicular Young's modulus, and (c) Ratio of parallel and perpendicular Young's modulus as a function of the dimensionless minimum gap ($2H_0/R$) for all material tested. Two different roll diameters were used: $2R = 0.01905$ m (close symbols) and $2R = 0.0762$ m (open symbols). Samples: (□,■) D-1102, (▲) 8550-D, (◆) B 20-80, (●) B 40-60, and (▼) B 60-40.

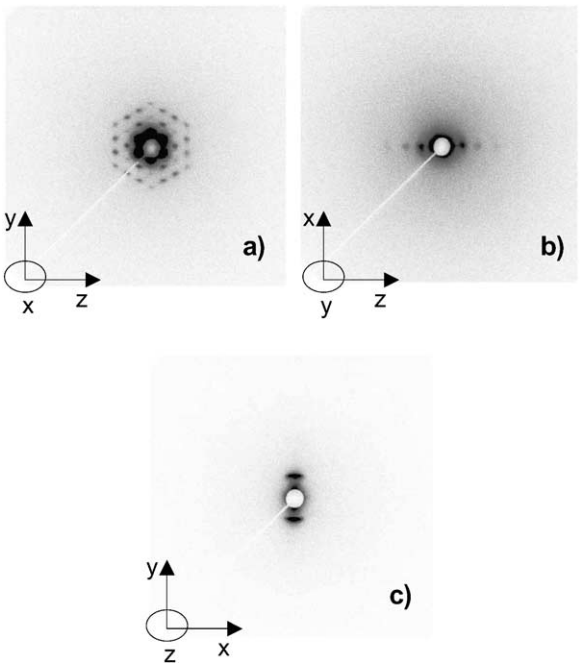

Fig. 5. SAXS patterns of a neat SBS roll-cast sample (DEXCO 8550-D, thickness = 0.00062 m) recorded with the X-ray beam perpendicular to (a) *zy*, (b) *zx*, and (c) *xy* planes. The first and second letter corresponds to the equatorial and meridional line of the pattern. Sample-detector distance is 0.4 m for (a) and 0.6 m for (b) and (c).

Fig. 5(b) is a representative pattern recorded maintaining the beam perpendicular to the film plane. Along with the q_1 reflection, the second reflection q_2 is well defined. The third X-ray pattern recorded with the beam along *z*-direction (Fig. 5(c)) preferentially shows only the first reflection q_1 for all the samples investigated. The differences observed between the last two patterns (Fig. 5(b) and (c)) would indicate a preferential alignment of the *a* axis along with the *z*-direction.

In order to compare the orientation of the samples we have obtained the variation of the intensity along circular profiles at the radius q_1, q_2, etc. Fig. 6 shows the intensity circular profiles recorded from the hexagonal pattern of a neat SBS (DEXCO 8550-D, thickness 0.62 mm). We have measured the full width at the half

Table 3
Variation of SAXS spacings d_1, d_2, and the hexagonal parameter *a* with blend composition

Sample	Processing method	Film thickness (mm)	$E_{\|}/E_{\perp}$	d_1 (nm)	d_2 (nm)	*a* (nm)
B 0-100	Simple cast	1.066	1.0	25.5	–	–
B 0-100	Roll-cast	0.62	28.8	26.2	15.3	30.6
B 20-80	Simple cast	0.985	1.0	25.8	–	–
B 20-80	Roll-cast	0.607	43.1	27.2	15.5	31.0
B 40-60	Simple cast	0.991	1.0	26.5	–	–
B 40-60	Roll-cast	0.584	43.7	28.8	17.2	34.3
B 60-40	Simple cast	1.015	1.0	30.1	–	–
B 60-40	Roll-cast	0.782	44.5	30.1	17.6	35.2
B 100-0	Simple cast	0.915	1.0	34.3	–	–

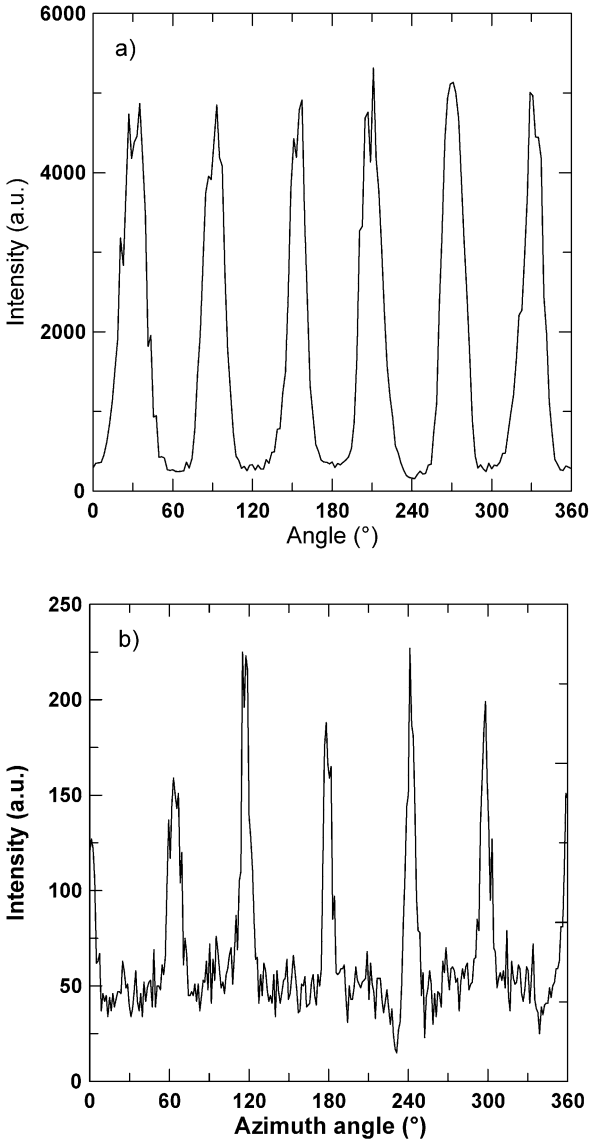

Fig. 6. SAXS intensity circular profiles recorded from the hexagonal pattern at the radial value of q_1 (a) and q_2 (b).

intensity maximum (FWHM) for each one of the six intensity profile peaks observed for q_1 and q_2. The obtained FWHM values, in degrees, from different X-ray patterns are shown in Table 4.

From the values of $\Delta\mu$ derived from the hexagonal X-ray pattern, the influence of diblock content on sample orientation is apparent. Cylinder orientation improves as the triblock SBS content increases. The degree of orientation derived from q_1, however, is lower than that from q_2. This could be attributed to some material, which scatter contributing only to q_1 but not to q_2 because of lack of crystal coherency. Concerning the orientation derived from the other two X-ray patterns (last two columns of Table 4) the FWHM values did not show any clear trend with SB content. However, both y and z directions are not equivalent from the orientation point of view.

Table 4
Average FWHM values (in degrees) for q_1 and q_2 reflections measured from SAXS intensity circle profiles in roll-cast samples. The first and second letter in parenthesis, referring to sample orientation, were maintained parallel to the equatorial and meridional line of the SAXS pattern, respectively

Sample	$\Delta\mu$		$\Delta\alpha$	
	q_1 (zy)	q_2 (zy)	q_1 (xy)	q_1 (zx)
B 0-100	14	7	17	19
B 20-80	17	8	20	13
B 40-60	19	10	15	33
B 60-40	23	14	22	13
B 100-0 (simple cast)	75	–	81	–

4. Conclusions

The ratio of parallel to perpendicular Young's modulus is almost constant for films prepared with a dimensionless minimum gap in the range of 0.02–0.09. Relative high values of either the pressure or the shear rate on the rolls surface when $2H_0/R$ is lower than approximately 0.02 can be responsible for the misorientation of cylinders in the macroscopic oriented samples.

The effect of diblock content on the orientation of samples was also studied from SAXS patterns. Blends of triblock and diblock with up to 60 wt% of diblock show orientation as good as the neat triblock. The parallel to perpendicular Young's modulus ratio as well as the FWHM of blends with different content of diblock are similar to the values obtained for the pure triblock. Blends with higher content of diblock as well as pure diblock cannot be investigated due to the lack of mechanical integrity, prohibiting removal of the film from the stainless steel roll.

Acknowledgments

We would like to thank Dr Dale Handlin at Kraton Co., and Brian Walther at DEXCO Co. for the material. We also want to thank Dr Ramon Albalak for the introduction to the roll-casting procedure. MAV gratefully acknowledges the fellowship support of the Consejo Nacional de Investigaciones Científicas y Técnicas (CONICET) of Argentina. This work was supported by AFOSR 91-0078 and DGYCT (Spain) project BFM2000-1474.

References

[1] Folkes MJ, Keller A, Scalisi FP. Colloid Polym Sci 1973;251:1–4.
[2] Keller A, Odell JA. In: Folkes M, editor. Process, structure and properties of block copolymers. London: Elsevier; 1985. chapter 2.
[3] Hadziioannou G, Mathis A, Skoulios A. Colloid Polym Sci 1979;257:136–9.
[4] Morrison FA, Winter HH. Macromolecules 1989;22:3533–40.

[5] Le Meur J, Terrisse J, Schwab C, Goldzene J. Phys (Paris), Colloq C5a 1971;32(10):301–4.
[6] Amundson K, Helfand E, Davis DD, Quan X, Patel SS, Smith SD. Macromolecules 1991;24:6546–8.
[7] Koppi KA, Tirrell M, Bates FS. Phys Rev Lett 1993;70:1449–52.
[8] Winter HH, Scott DB, Gronski W, Okamoto S, Hashimoto T. Macromolecules 1993;26:7236–44.
[9] Rangaramanujam MK, Kornfield JA. Macromolecules 1994;27:1177–86.
[10] Rosedale JH, Bates FS, Almdal K, Mortensen K, Wignall GD. Macromolecules 1995;28:1429–43.
[11] Pinheiro BS, Hajduk DA, Gruner SM, Winey KI. Macromolecules 1996;29:1482–9.
[12] Gupta VK, Krishnamoorti R, Chen Z-R, Kornfield JA, Smith SD, Satkowski MM, Grothaus JT. Macromolecules 1996;29:875–84.
[13] Laurer JH, Pinheiro BS, Polis DL, Winey KI. Macromolecules 1999;32:4999–5003.
[14] Polis DL, Smith SD, Terrill NJ, Ryan AJ, Morse DC, Winey KI. Macromolecules 1999;32:4668–76.
[15] Bates FS, Koppi KA, Tirrell M, Almdal K, Mortensen K. Macromolecules 1994;27:5934–6.
[16] Tepe T, Schulz MF, Zhao J, Tirrell M, Bates FS, Mortensen K, Almdal K. Macromolecules 1995;28:3008–11.
[17] Albalak RJ, Thomas EL. J Polym Sci, Polym Phys 1993;31:37–46.
[18] Albalak RJ, Thomas EL. J Polym Sci, Polym Phys 1994;32:341–50.
[19] Albalak RJ, Thomas EL, Capel MS. Polymer 1997;38:3819–25.
[20] Albalak RJ, Capel MS, Thomas EL. Polymer 1998;39:1647–56.
[21] Fetters LJ. Exxon Co., private communication.
[22] Eisen A. BS Thesis, Massachusetts Institute of Technology; 1999.
[23] Odell JA, Keller A. Polym Engng Sci 1985;17:544–59.
[24] Honeker CC, Thomas EL. Chem Mater 1996;8:1702–14.
[25] Honeker CC, Thomas EL, Albalak RJ, Hajduk DA, Gruner SM, Capel MC. Macromolecules 2000;33:9395–406.